



# *Scyntylatory do detekcji neutronów*

**Łukasz Świdorski**

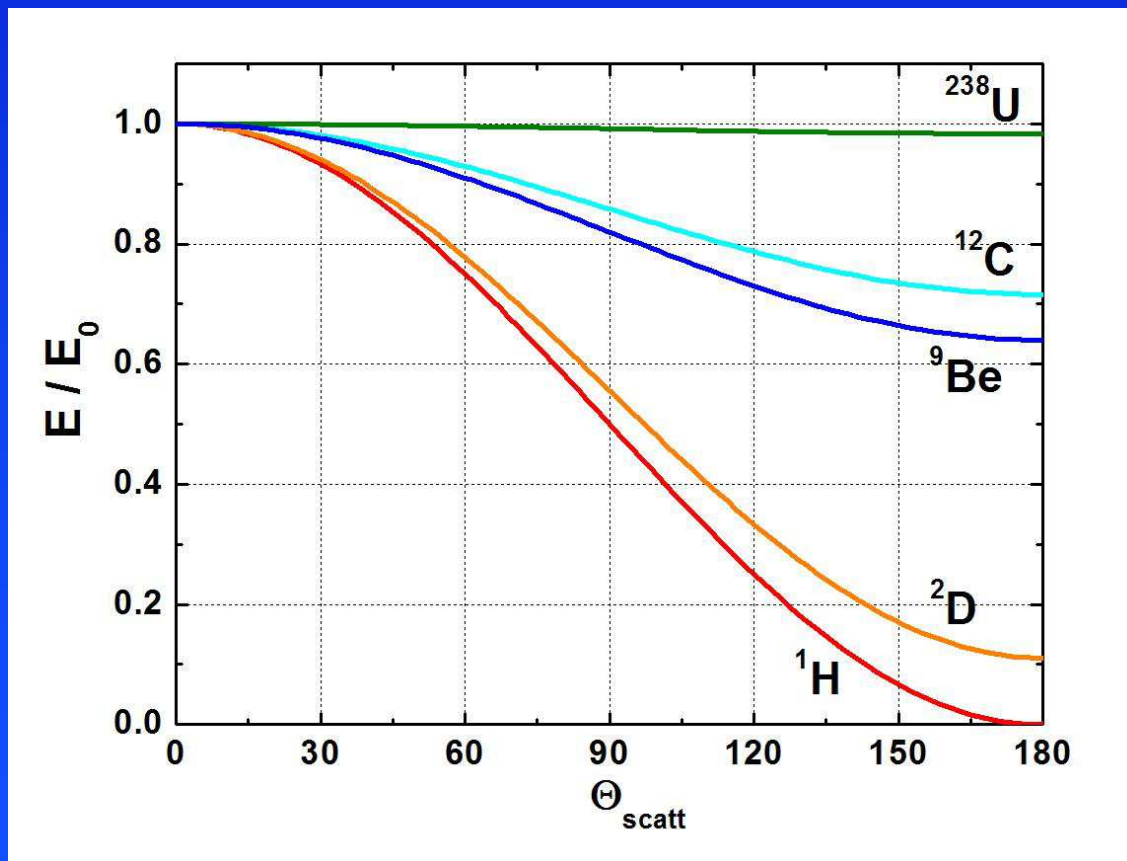
*Narodowe Centrum Badań Jądrowych  
Departament Technik Jądrowych i Aparatury  
Zakład Fizyki Detektorów (TJ3)  
ul. Sołtana 7  
05-400 Otwock-Świerk*

# 1. Metody detekcji neutronów



**Neutrony prędkie:**  
rozpraszanie  
elastyczne

$$\frac{E}{E_0} = \frac{1}{2} \left\{ 1 + \left( \frac{A-1}{A+1} \right)^2 + \left[ 1 - \left( \frac{A-1}{A+1} \right)^2 \right] \cos \Theta_{\text{scatt}} \right\}$$



dla <sup>1</sup>H:

$$\frac{E}{E_0} = \frac{1 + \cos \Theta_{\text{scatt}}}{2}$$

# 1. Metody detekcji neutronów



**Neutrony prędkie:**  
rozpraszanie nieelastyczne  
- reakcje  $(n, n'\gamma)$   
- reakcje  $(n, p)$  i  $(n, \alpha)$   
prowadzące do rozpadu  $\beta^-$

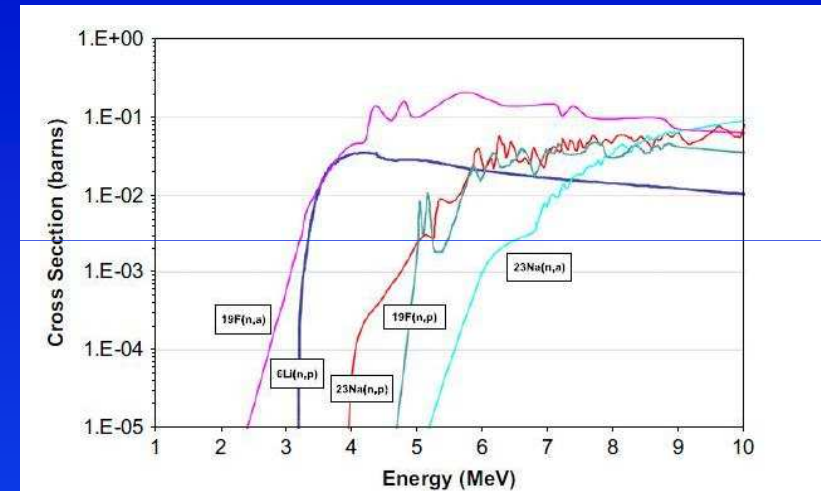


Fig. 2. Fast neutron cross-sections for threshold activation reactions in some TAD materials.

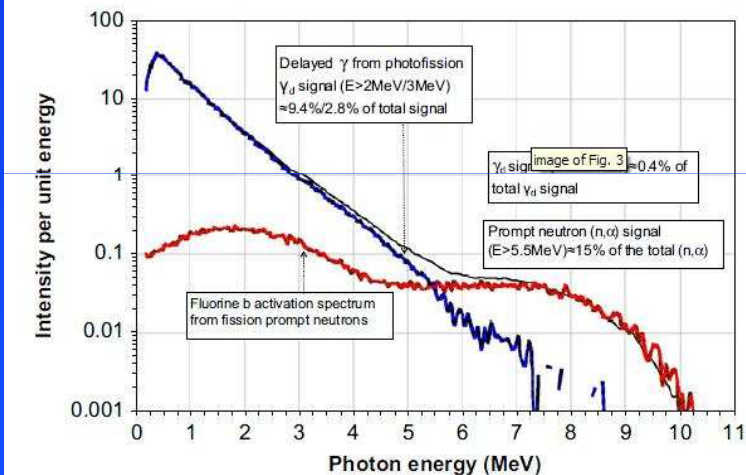


Fig. 3. Fission prompt neutrons and delayed gamma rays as detected in FC detector between short pulses of 9 MV Bremsstrahlung X-rays.

T. Gozani *et al.*, NIM A652 (2010) 334-337  
„Neutron threshold activation detectors  
(TAD) for the detection of fissions”

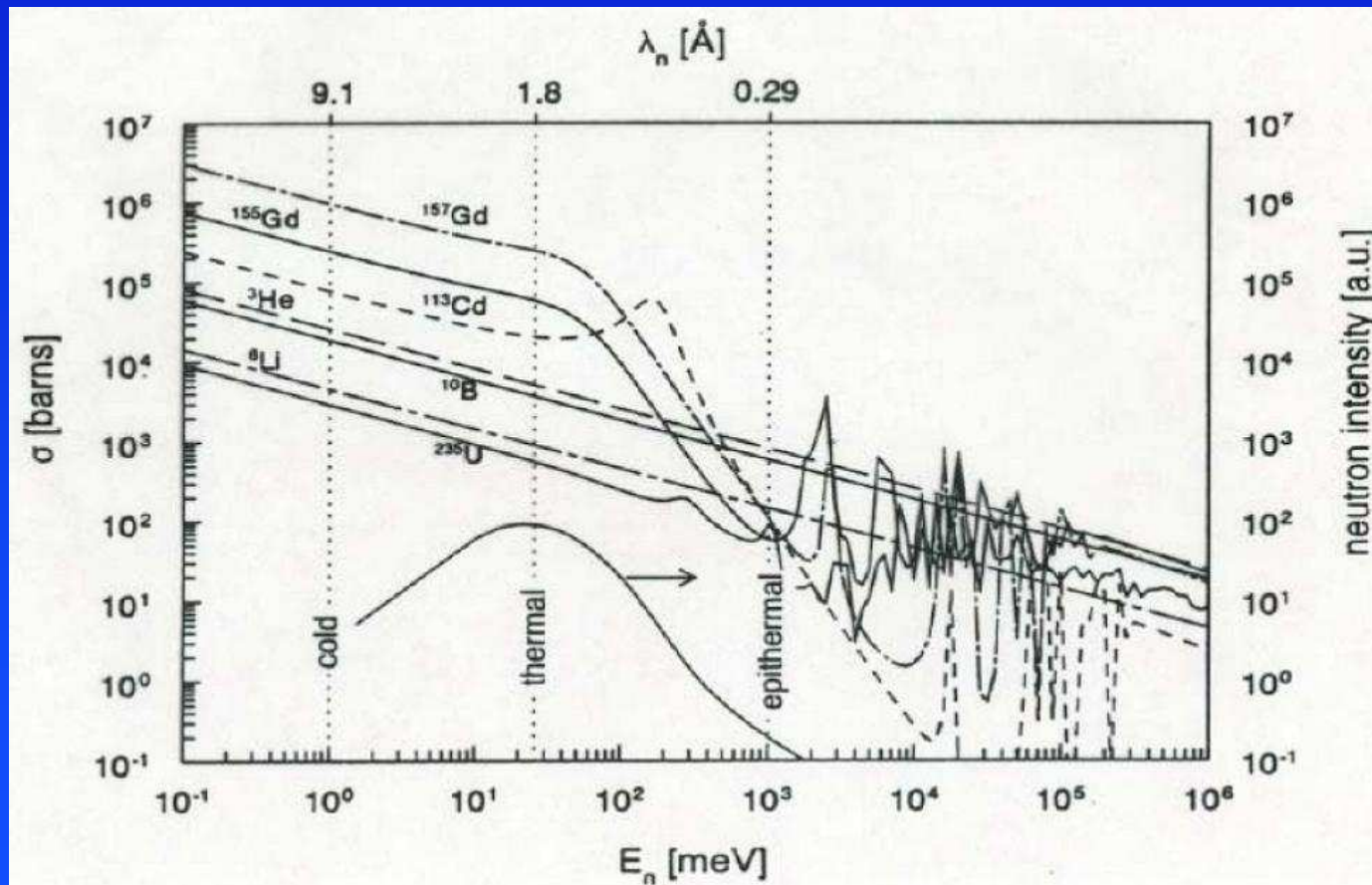


## Neutrony wolne – wychwyty na:

- He-3       ${}^3\text{He} + n \rightarrow p + {}^3\text{H}$       (Q = 764 keV)
- Li-6       ${}^6\text{Li} + n \rightarrow \alpha + {}^3\text{H}$       (Q = 4.8 MeV)
- B-10       ${}^{10}\text{B} + n \rightarrow \alpha + {}^7\text{Li} + \gamma$  (482 keV)      (Q = 2.3 MeV)
- Gd-157       ${}^{157}\text{Gd} + n \rightarrow {}^{158}\text{Gd} + \gamma$  ( $\Sigma = 8$  MeV)  
                  ${}^{157}\text{Gd} + n \rightarrow {}^{158}\text{Gd} + \text{Ce}^-$  (72 keV)
- Cd-113       ${}^{113}\text{Cd} + n \rightarrow {}^{114}\text{Cd} + \gamma$  ( $\Sigma = 9$  MeV)



## Neutrony wolne – przekrój czynny na wychwyty:

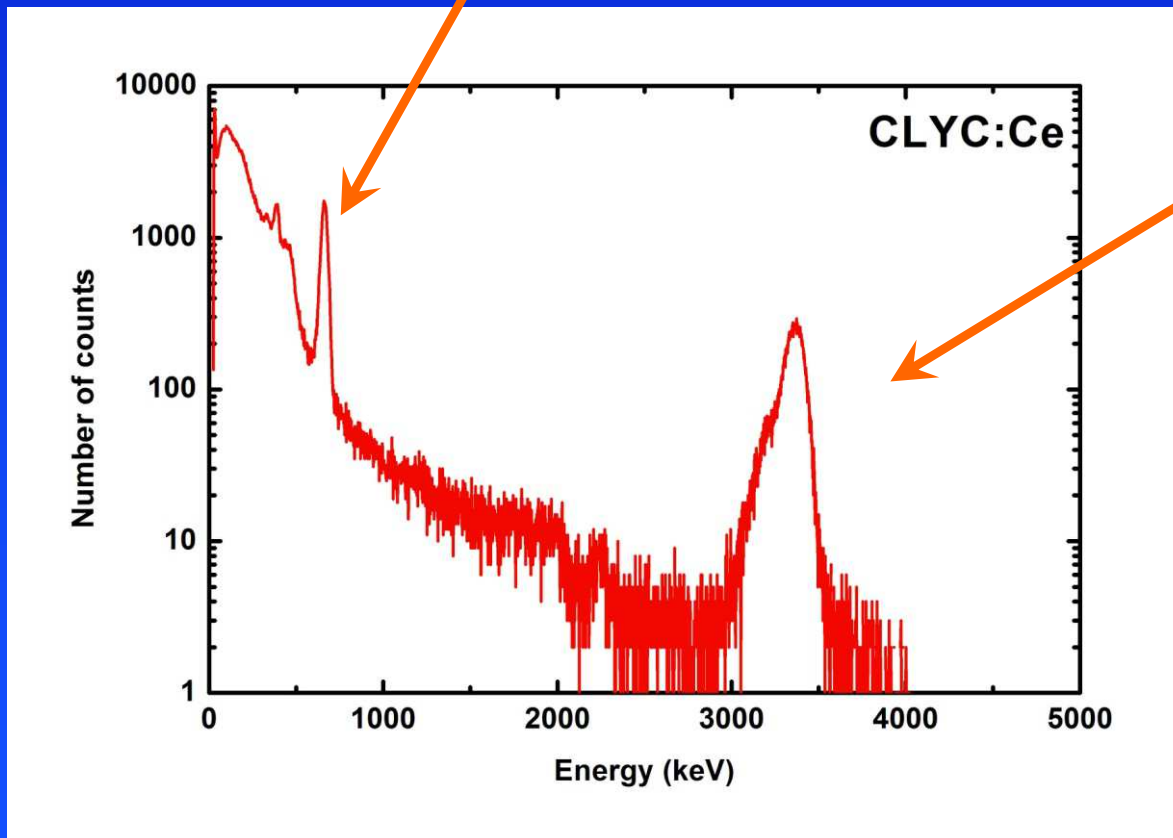




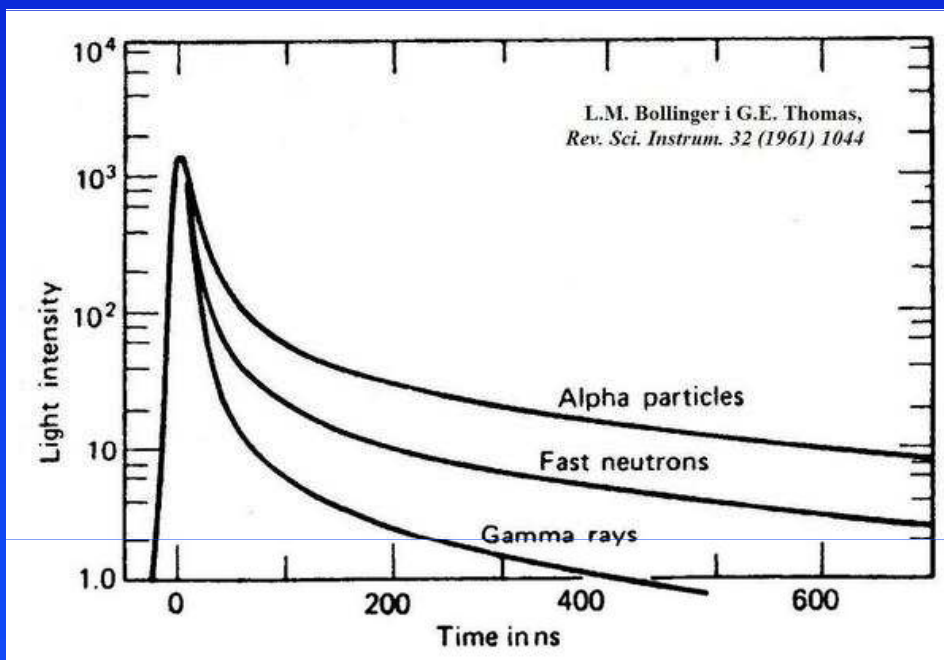
### Pulse Height Discrimination (PHD)

662 keV  $\gamma$ -rays

${}^6\text{Li} + n$



# Pulse Shape Discrimination (PSD) charge integration (CI)



S.D. Clarke *et al.*, NIM A604 (2009) 618-623  
„Neutron and gamma-ray cross-correlation  
measurements of plutonium oxide powder”

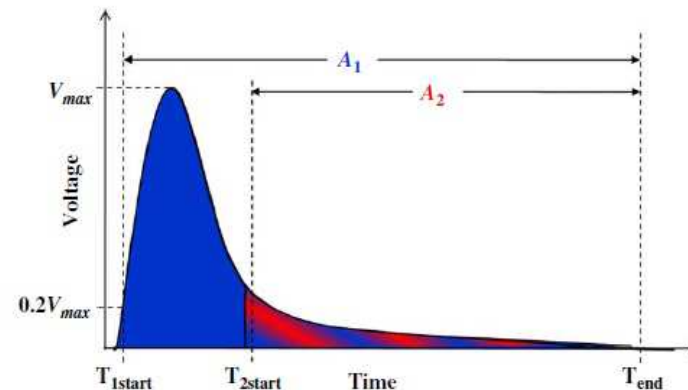


Fig. 2. Illustration of the pulse shape obtained from the EJ-309 liquid scintillator. The total integral ( $A_1$ ) and tail integral ( $A_2$ ) are computed for each pulse and used for classification as a neutron or gamma ray. Pulse timing was achieved by measuring the time at which the pulse reaches 20% of the pulse amplitude.

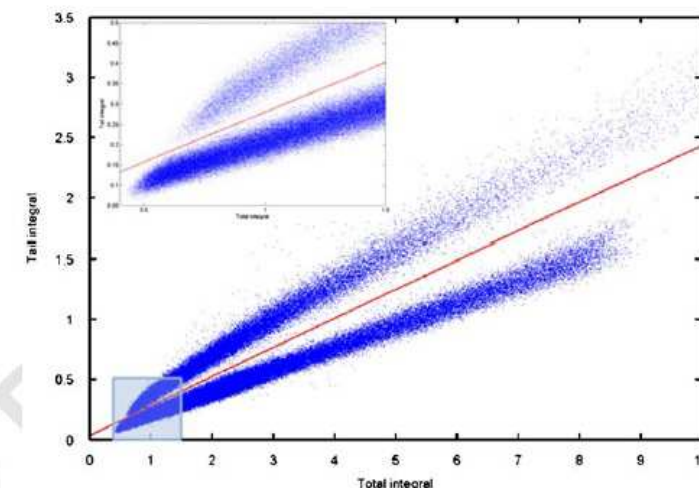
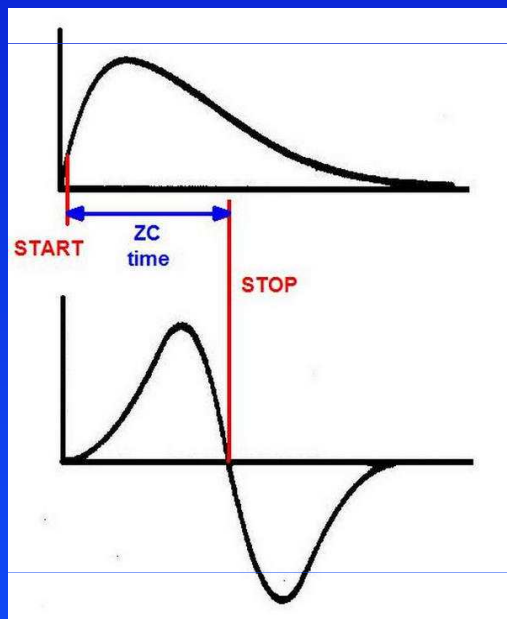
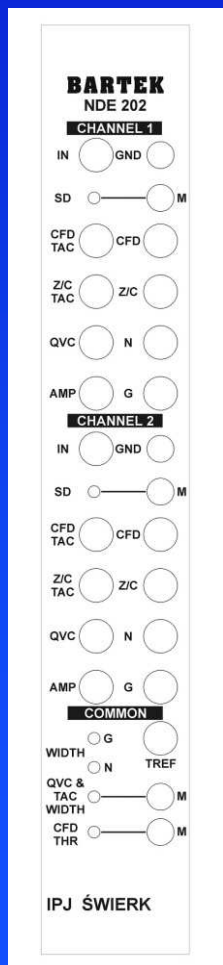


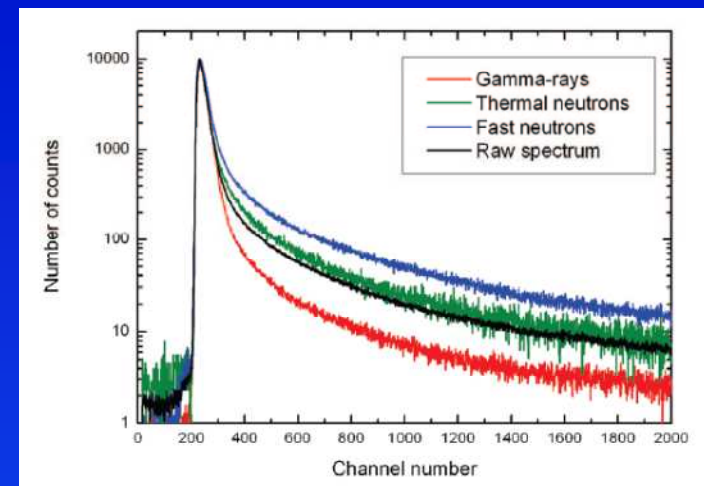
Fig. 3. Tail and total pulse integrals for measured pulses from a 500-g, low-burnup  $PuO_2$  sample. The discrimination line is shown: pulses above the line are classified as neutrons and below the line as gamma rays. The low-energy region is shown in the inset.



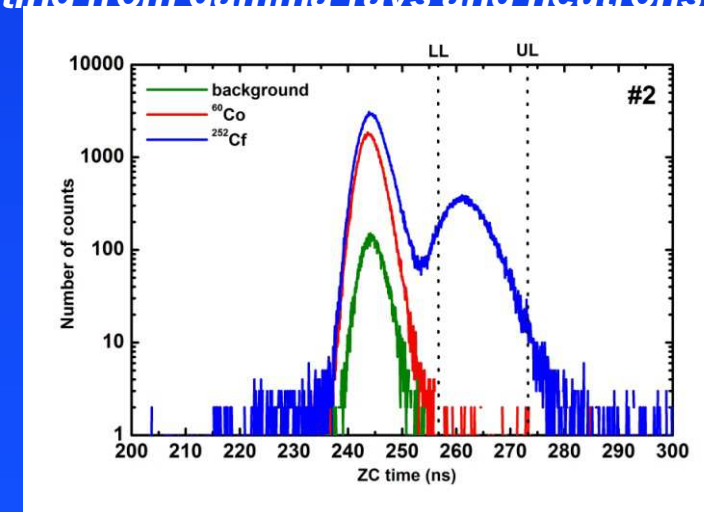
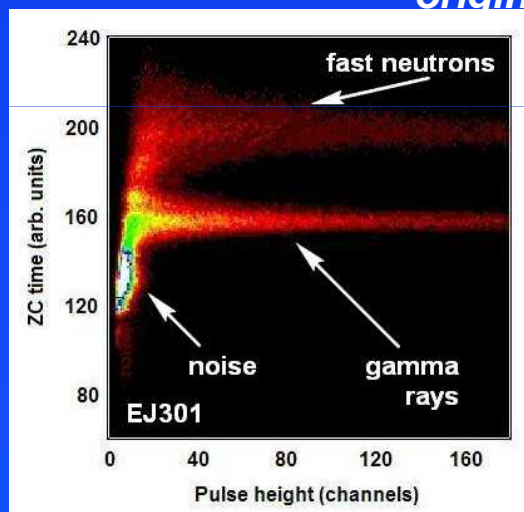
# Pulse Shape Discrimination (PSD) zero-crossing (ZC)



EUROBALL  
 Neutron  
 Detector  
 Electronics  
 BARTEK NDE 202



T. Szcześniak *et al.*, TNS 57 (2010) 3846-3852  
 „Light pulse shapes in liquid scintillators  
 originating from gamma-rays and neutrons”







### Pulse Shape Discrimination ZC vs CI

$$FOM = \frac{centr_n - centr_\gamma}{FWHM_\gamma + FWHM_n}$$

D. Wolski *et al.*, NIM A360 (1995) 584-592  
„Comparison of n-γ discrimination by  
zero-crossing and digital charge  
comparison methods”

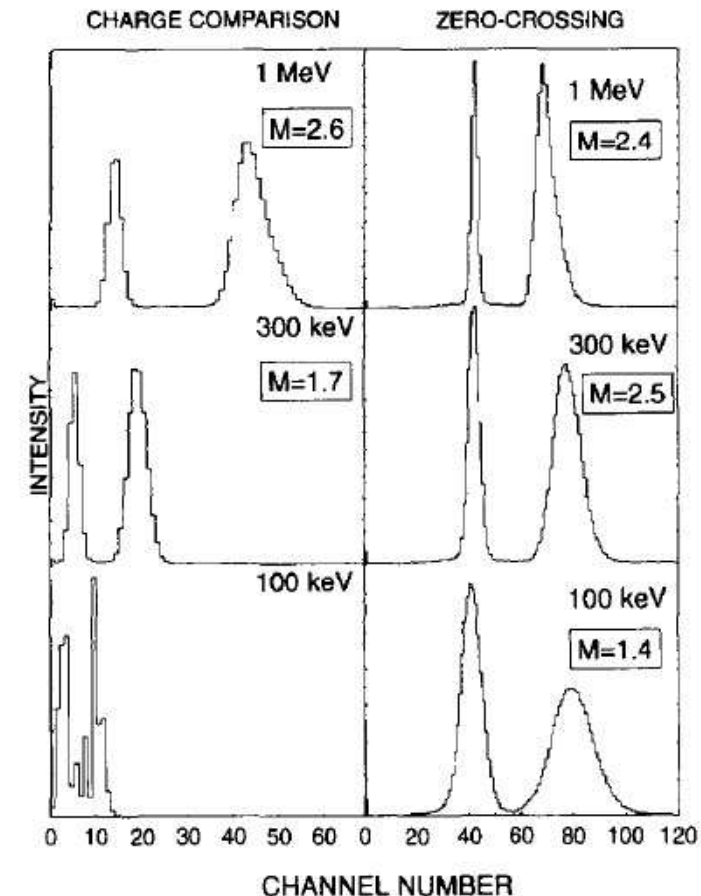


Fig. 6. Comparison of the n-γ discrimination spectra for gates set at 1 MeV, 300 keV and 100 keV selected from the 2D spectra presented in Fig. 5 for the charge comparison (left) and the zero-crossing (right) methods respectively.

### 3. Scyntylatory: plastiki



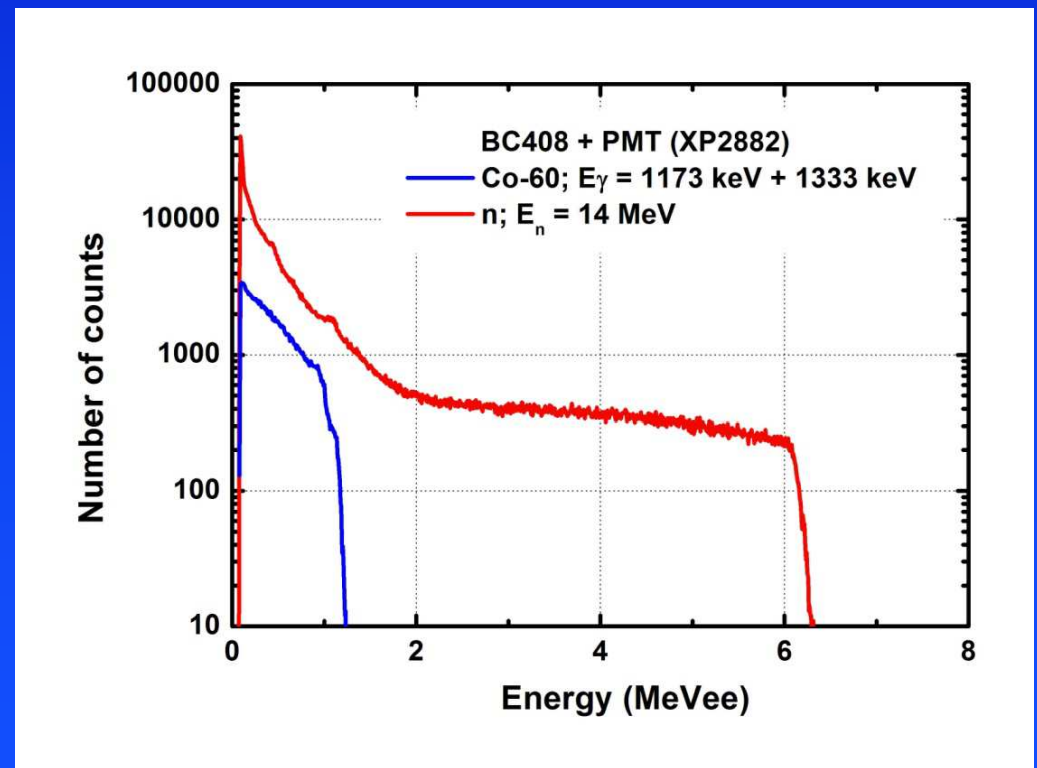
**BC408**

Saint-Gobain Crystals

plastik 5x5x5 mm<sup>3</sup> + fotopowielacz

neutrony – rozpraszanie elastyczne, zasięg protonów odrzutu ~ $\mu\text{m}$

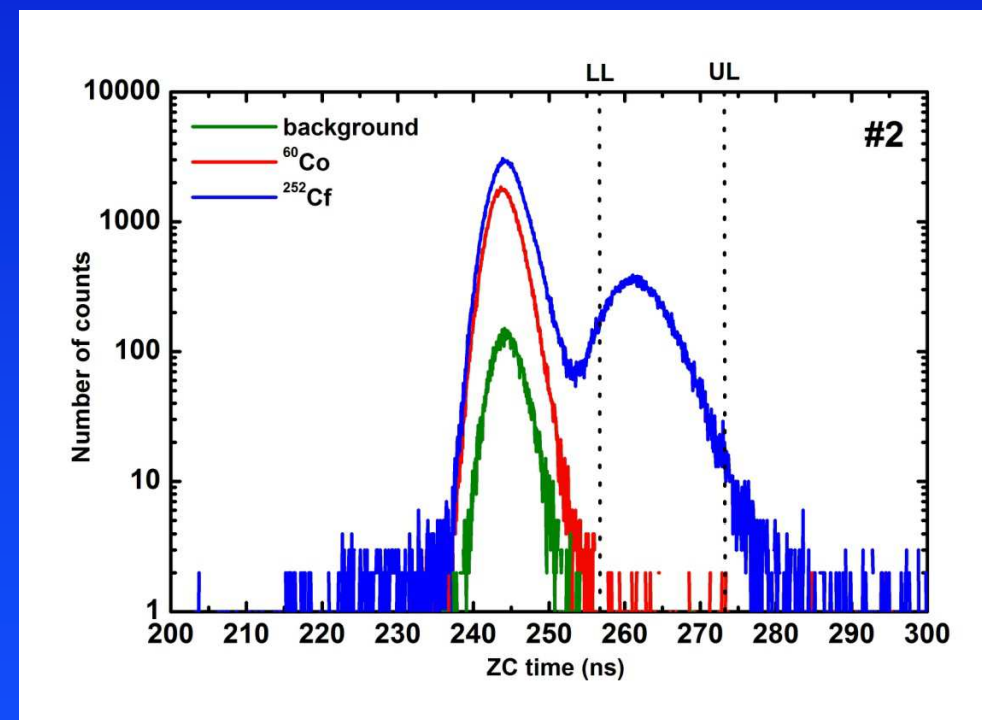
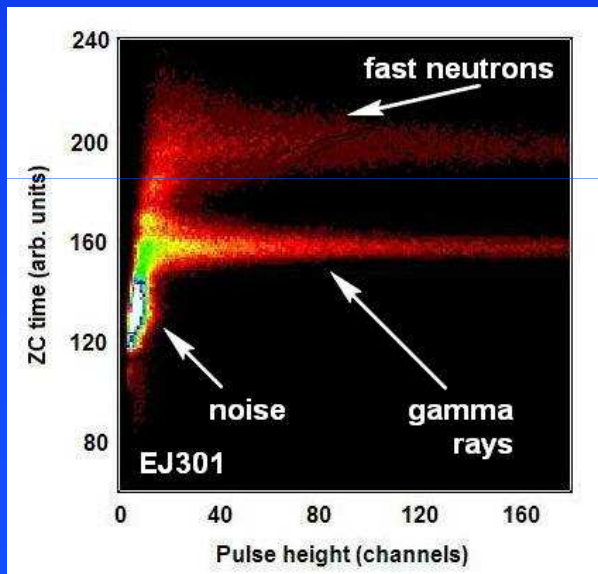
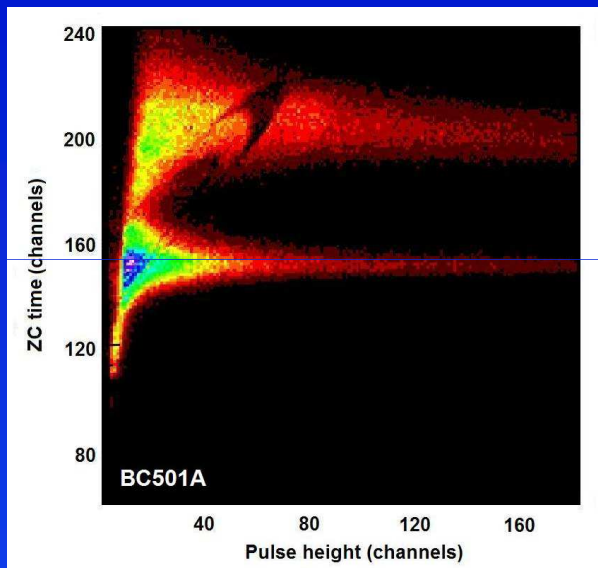
elektrony – rozpraszanie Comptona, zasięg elektronów odrzutu ~mm





## BC501-EJ301-NE213

Saint-Gobain Crystals

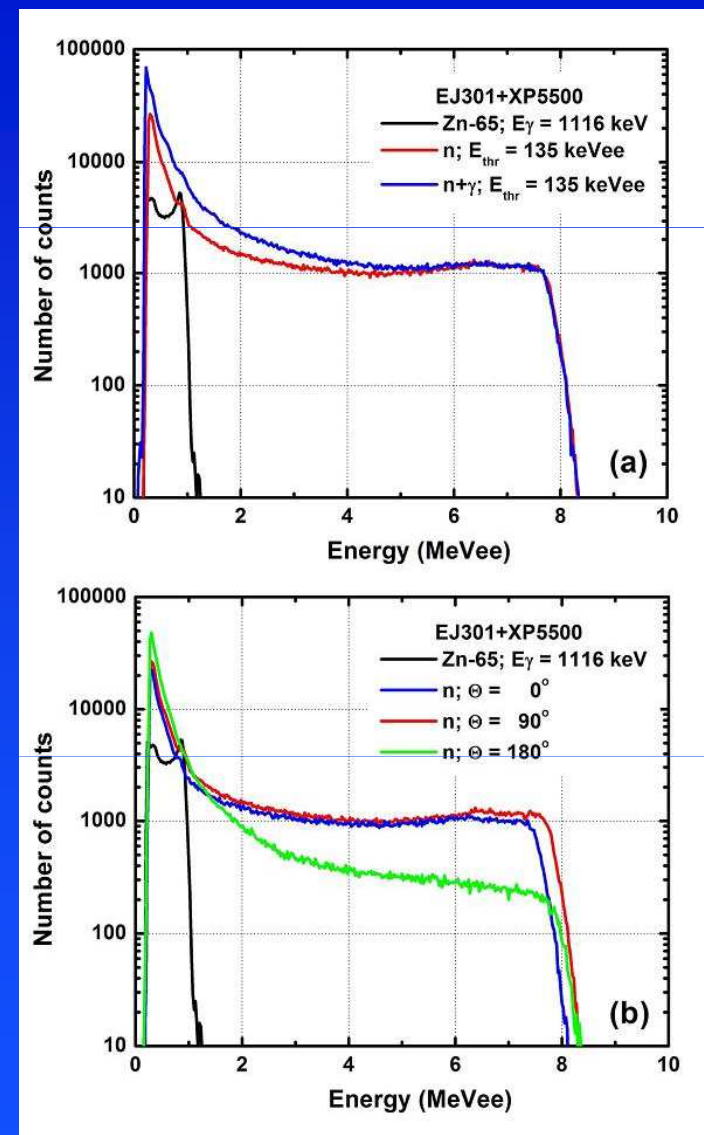
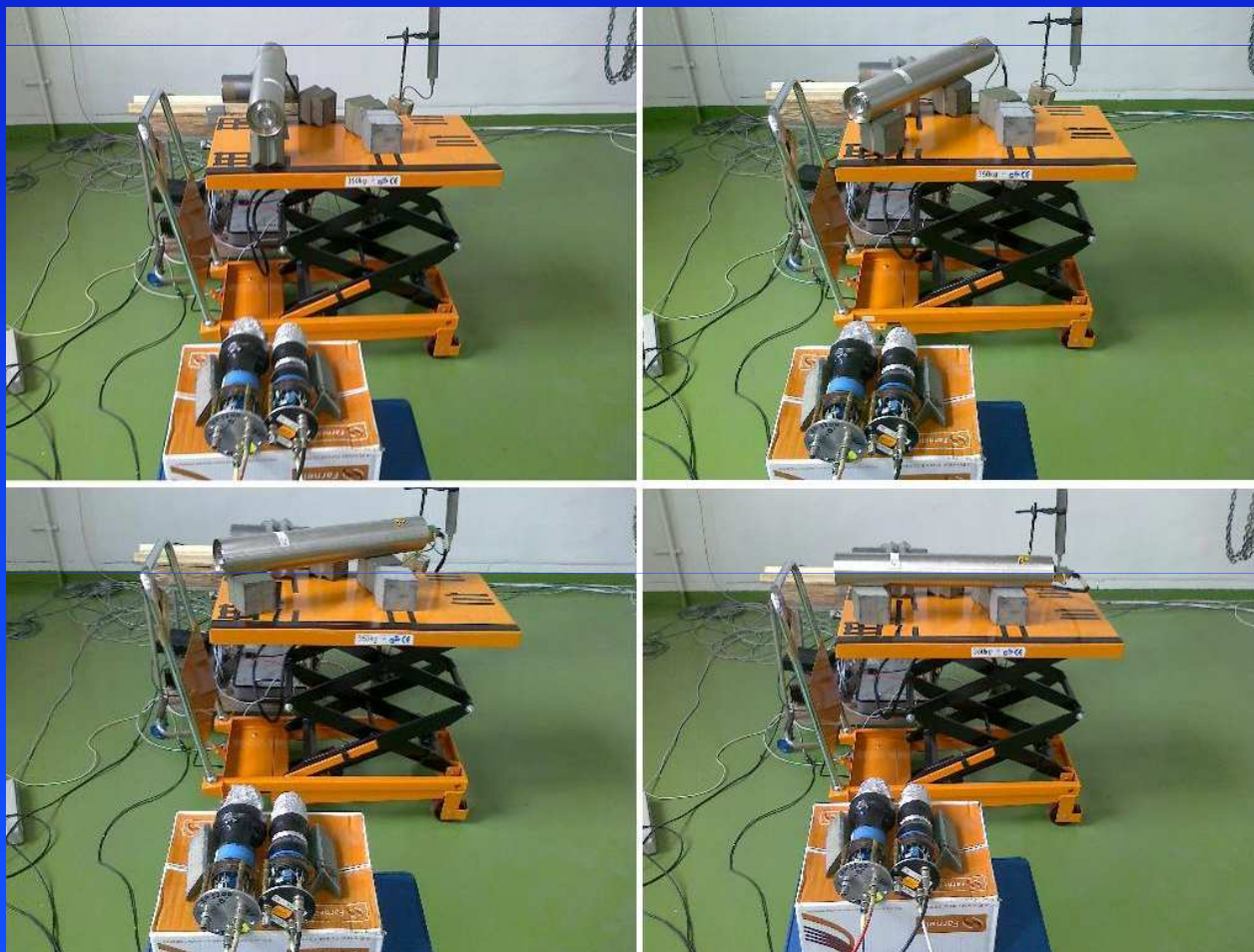


Scionix Holland B.V. / Eljen Technologies Inc.



## EJ301

Scionix Holland B.V. / Eljen Technologies Inc.

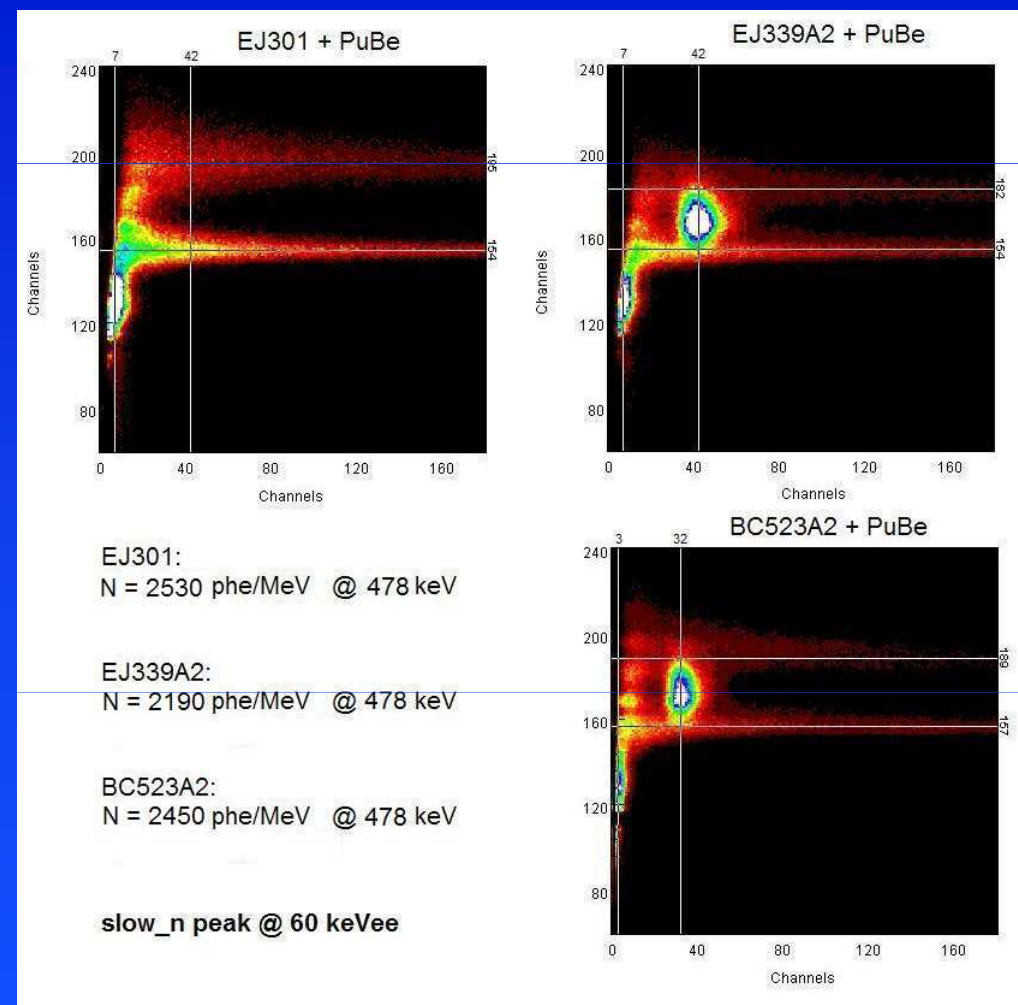
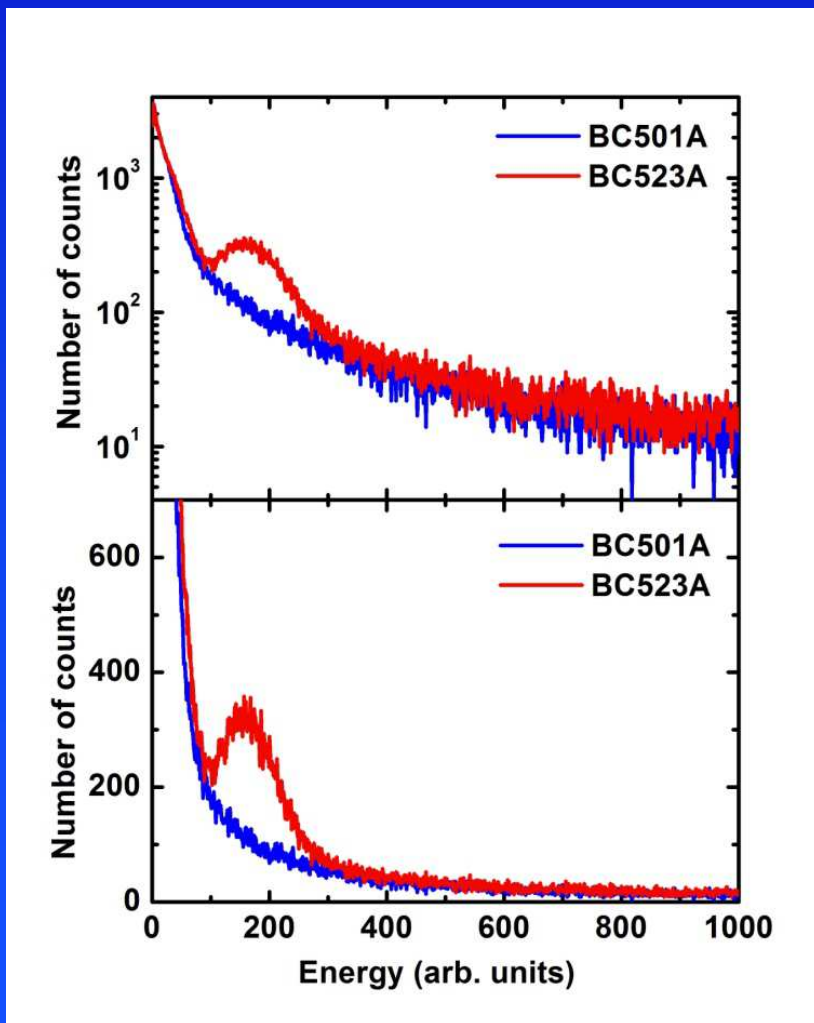


### 3. Scyntylatory: ciekłe scyntylatory



Scionix Holland B.V. / Eljen Technologies Inc.

## BC523A2-EJ339A2

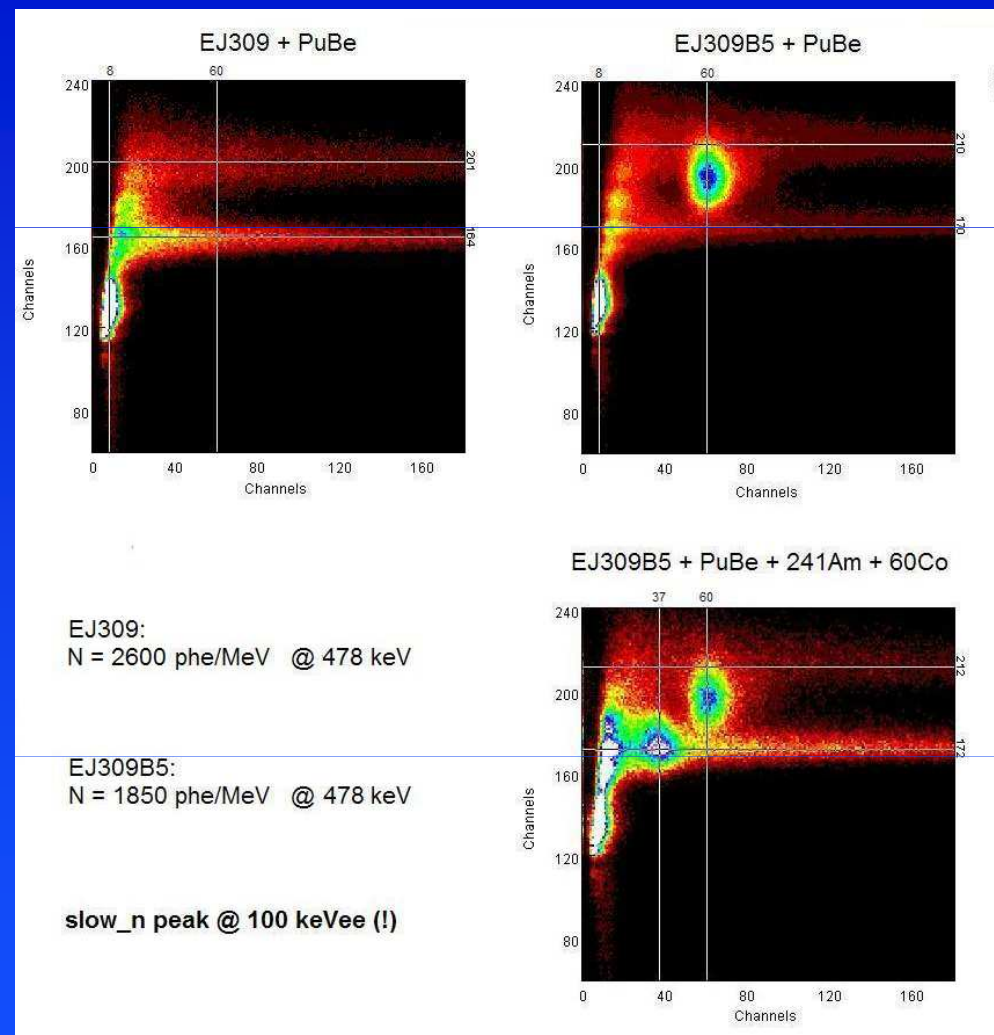
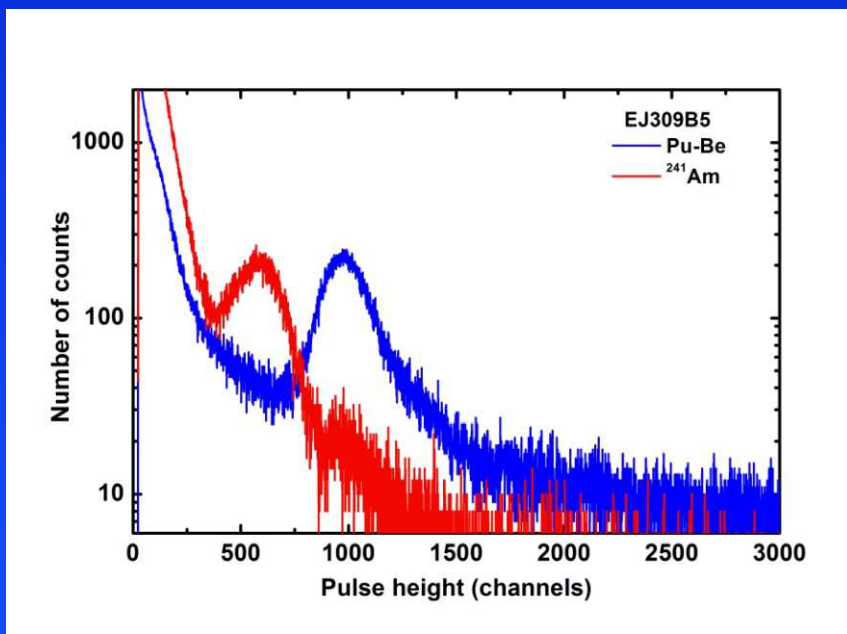


Saint-Gobain Crystals



## EJ309-EJ309B5

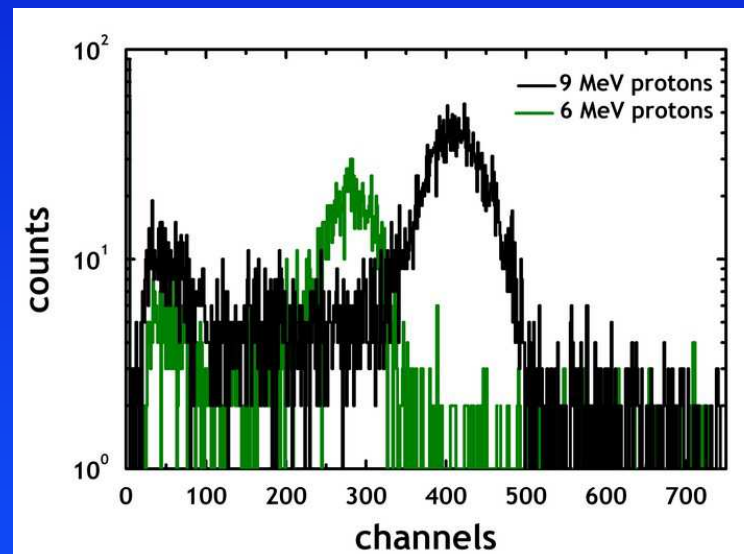
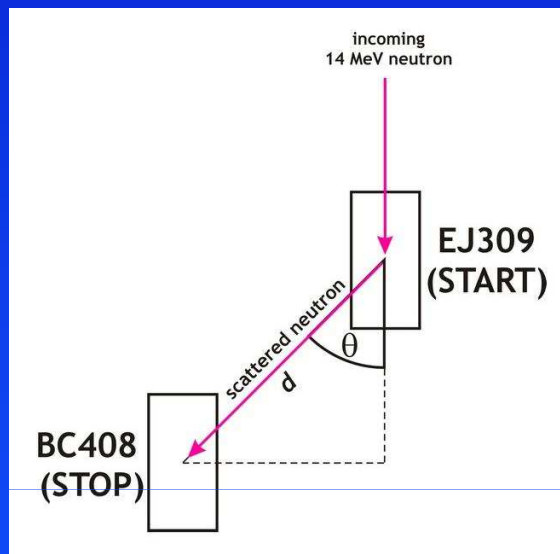
ciekły scyntylator  
wysokotemperaturowy



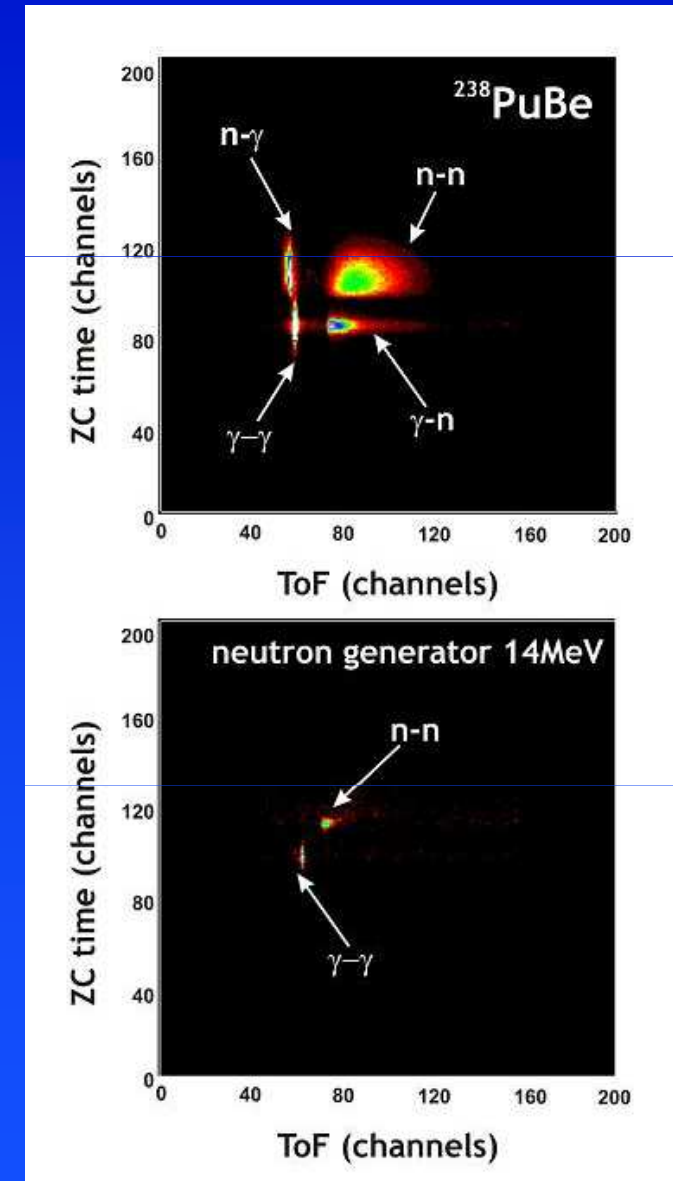
Scionix Holland B.V. / Eljen Technologies Inc.



## EJ309: kalibracja energetyczna odpowiedzi na neutrony

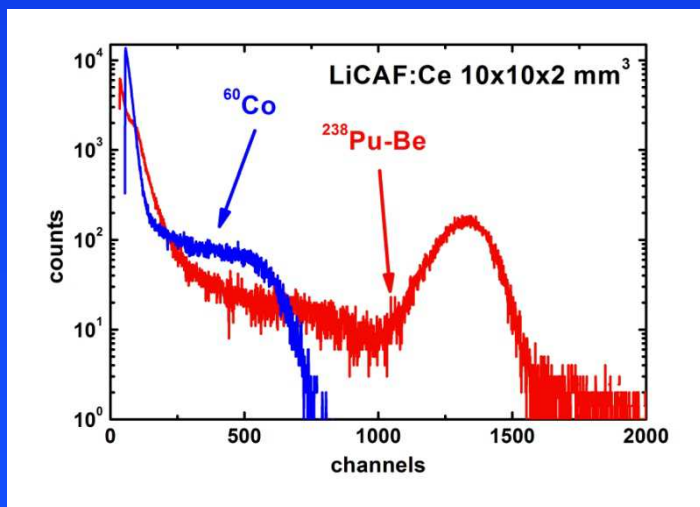
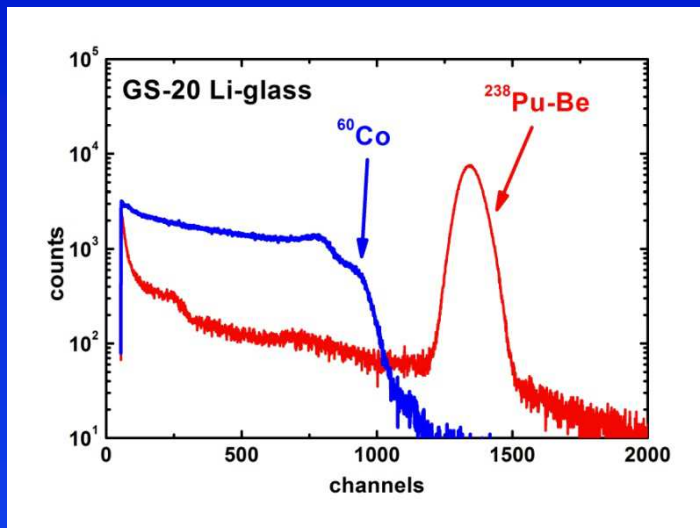


J. Iwanowska et al., 2012 IEEE NSS-MIC Conf. Rec. N1-67  
„Calibration of EJ309 liquid scintillator for neutron  
spectrometry”





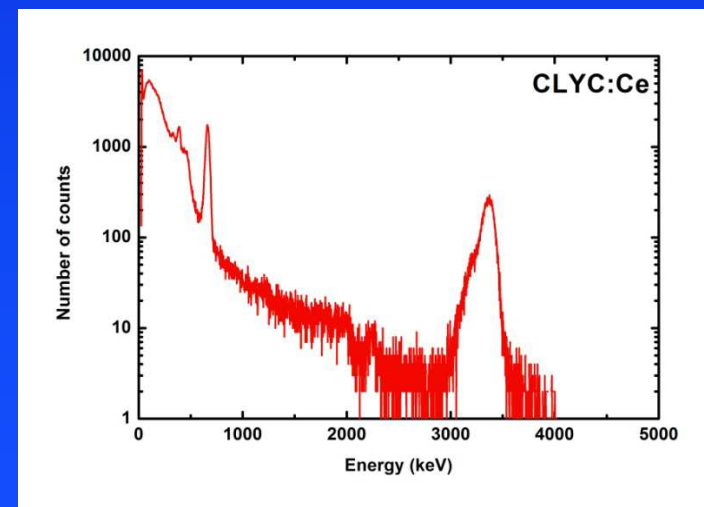
## Saint-Gobain Crystals



Tokuyama

## GS-20 - LiCAF:Ce – CLYC:Ce

J. Iwanowska et al., NIM A652 (2011) 319-322  
„Thermal neutron detection with Ce<sup>3+</sup> doped  
LiCaAlF<sub>6</sub> single crystals”



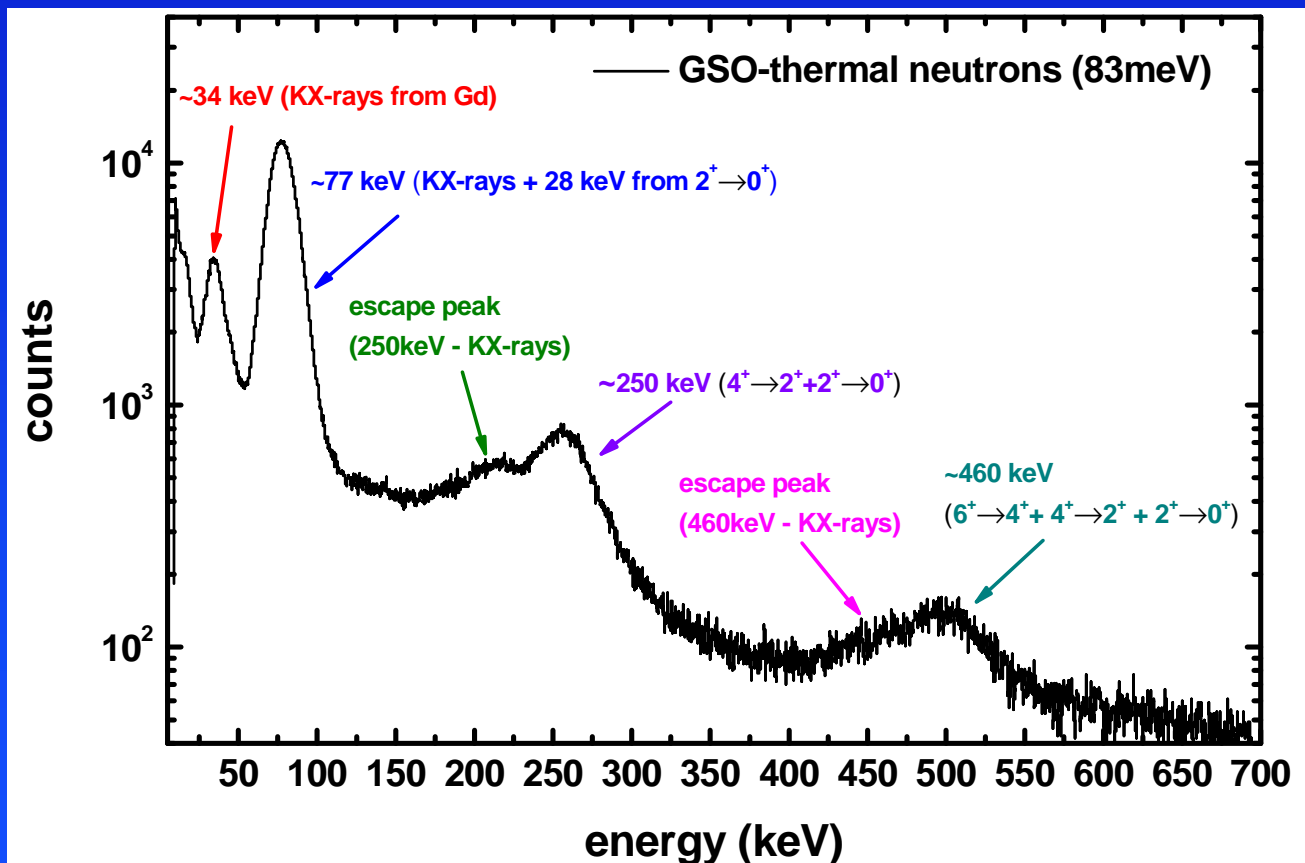
RMD Inc. / FLIR Radiation GmbH





## GSO:Ce – GAGG:Ce

detekcja elektronów konwersji wewnętrznej





**He-4 gas scintillator:**  
**p = 200 bar (!)**  
**low  $\gamma$ -ray sensitivity**  
**n/ $\gamma$  discrimination**

**Jinst** PUBLISHED BY IOP PUBLISHING FOR SISSA MEDIALAB

RECEIVED: January 9, 2012  
ACCEPTED: February 20, 2012  
PUBLISHED: March 19, 2012

2<sup>nd</sup> INTERNATIONAL WORKSHOP ON FAST NEUTRON DETECTORS AND APPLICATIONS,  
NOVEMBER 6–11 2011,  
EIN GEDI, ISRAEL

### Fast neutron detection with pressurized <sup>4</sup>He scintillation detectors

R. Chandra,<sup>a,1</sup> G. Davatz,<sup>a,b</sup> H. Friederich,<sup>a,b</sup> U. Gendotti<sup>a</sup> and D. Murer<sup>a,b</sup>

<sup>a</sup>Arktis Radiation Detectors Ltd,  
Technoparkstrasse 1, 8005 Zurich, Switzerland  
<sup>b</sup>ETH Zurich, Institute for Particle Physics,  
Schafmattstrasse 20, 8093 Zurich, Switzerland

E-mail: rico.chandra@arktis-detectors.com

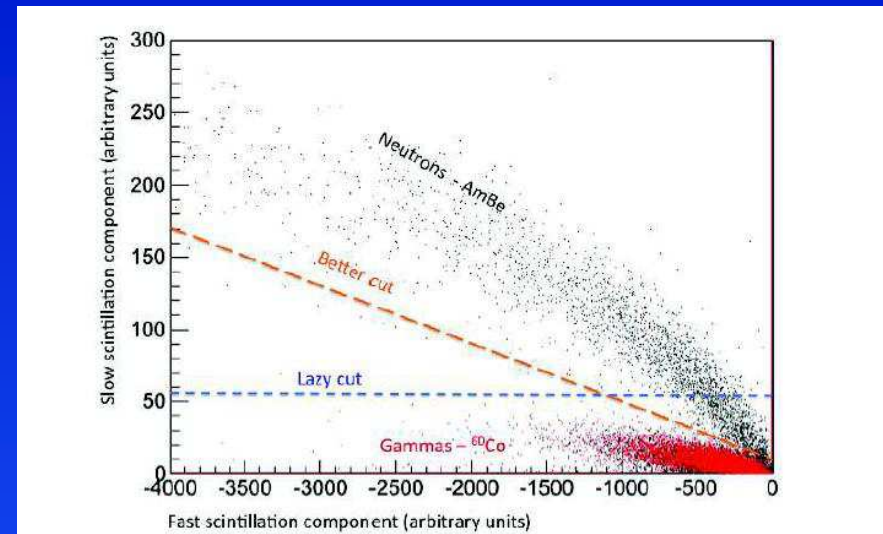


Figure 4. Scintillation signals from neutron interactions can be distinguished from gamma interactions on the basis of the larger ratio of photons in the slow scintillation component. The dotted lines notionally show the cuts described in the text.

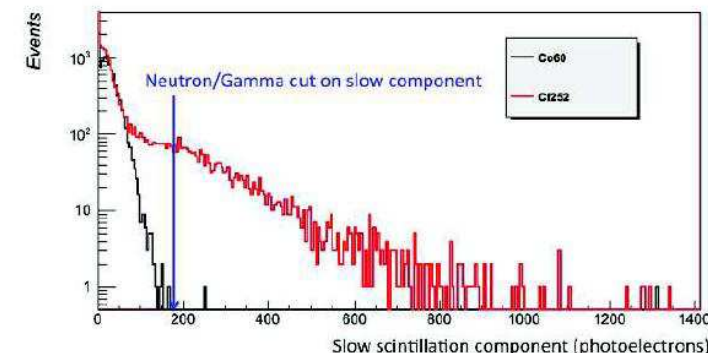


Figure 5. Histogram of the number of detected slow component photons from a <sup>60</sup>Co gamma source placed in contact with the detector (black entries) and a <sup>252</sup>Cf source (red entries). The “lazy cut” sacrifices neutron detection efficiency.



### Scyntylatory do detekcji neutronów

#### Kryształy

- CLYC:Ce
- Lil:Eu
- GSO:Ce
- GAGG:Ce

#### Ciekłe scyntylatory

- BC501A-EJ301
- BC523A-EJ339A (B-10 loaded)
- EJ309 (high flash point)
- EJ309B5 (B-10 loaded)
- EJ-313 (Fluorine Carbon)

#### Plastiki

- BC408
- EJ299 (z rozróżnianiem n/g!)
- stilbene, p-terphenyl (kompozyty)
- GS-20 (szkło scyntylacyjne)

#### Scyntylatory Gazowe

- He-4



**Dziękuję za uwagę!**

